Mechanism of Nitrous Oxide Formation by Metal-Catalyzed Reduction of Nitric Oxide in Aqueous Solution

Joseph H. MacNeil, Polly A. Berseth, Eric L. Bruner, Temur L. Perkins, Yasmine Wadia, Glenn Westwood, and William C. Trogler*

Contribution from the Department of Chemistry and Biochemistry, University of California at San Diego, La Jolla, California 92093-0358

Received October 15, 1996[⊗]

Abstract: Kinetics data were collected for the palladium-catalyzed reduction of nitric oxide (NO) to nitrous oxide (N_2O) with cuprous chloride reductant in 2 M hydrochloric acid ($2NO + 2CuCl + 2HCl \rightarrow N_2O + 2CuCl_2 + H_2O$). The rate-determining step was first order in the palladium concentration and NO partial pressure. The cuprous chloride dependence was first order below 0.1 M; at higher concentrations saturation kinetics were observed. The rate of reaction was independent of H^+ and Cl^- concentrations. Kinetics results were consistent with the initial, reversible attack (k_1/k_{-1}) of free NO on the bound nitrosyl of $[PdCl_3NO]^{2-}$ yielding $[PdCl_3(N_2O_2)]^{2-}$, which is then reduced by Cu(I) (k_2) to generate products and recycle the palladium. A k_1 value of $(6.0 \pm 0.4) \times 10^{-6}$ $(P_{NO})^{-1}$ s^{-1} at 20 °C was calculated, with a k_{-1}/k_2 ratio of 0.116 ± 0.004 M. Rate measurements show that NO reduction by Cu(I) is the rate-limiting step in the Wacker-style catalysis of the $CO + 2NO \rightarrow CO_2 + N_2O$ reaction. The current mechanism resembles the nitric oxide reductase activities of cytochrome *c* oxidases, which proceed by Cu(I) reduction of a heme bound nitrosyl, and cytochrome P450nor.

Introduction

Nitric oxide is a ubiquitous byproduct of high-temperature combustion, and the development of abatement techniques remains a challenge. Attention has focused on the use of heated metal zeolites, such as Cu-ZSM-5, as heterogeneous catalysts for converting NO directly to N_2 and O_2.[1] Other approaches, such as selective catalytic reduction (SCR), add a reductant (NH_3) into the effluent stream, but this involves additional expense and complexity.[2]

Concomitant reduction of nitric oxide and oxidation of carbon monoxide can remove these noxious components from exhaust gases. Both eqs 1 and 2 are favored thermodynamically, but are kinetically inert in the absence of external catalysts.[3]

$$CO + 2NO \rightarrow CO_2 + N_2O \quad (1)$$

$$2CO + 2NO \rightarrow 2CO_2 + N_2 \quad (2)$$

Heterogeneous catalysts lower the thermal threshold for these reactions,[4] and several homogeneous catalysis systems have been identified that facilitate eq 1 at room temperature.[5−7] One of the simplest and fastest of the homogeneous catalyst systems employs $PdCl_2$ and $CuCl_2$ in aqueous hydrochloric acid.[5] The catalysis was interpreted as being analogous to the Wacker process, and simplified to the following net reactions:[8]

$$PdCl_2 + CO + H_2O \rightarrow Pd(0) + CO_2 + 2HCl \quad (3)$$

$$Pd(0) + 2NO + 2HCl \rightarrow PdCl_2 + N_2O + H_2O \quad (4)$$

$$Pd(0) + 2CuCl_2 \rightarrow PdCl_2 + 2CuCl \quad (5)$$

$$2CuCl + 2NO + 2HCl \rightarrow N_2O + 2CuCl_2 + H_2O \quad (6)$$

It was recognized that the mechanism for the production of nitrous oxide was more complex than the net reactions implied.[5] A UV/vis spectroscopic intermediate was observed during catalysis. Reaction 6 is too slow to account for the rapid rate of nitrous oxide production and eq 5 occurs much faster than eq 4.

Mechanisms of nitrous oxide formation are also of possible environmental significance. Atmospheric nitrous oxide concentrations are steadily increasing, and neither biotic nor anthropogenic sources of N_2O have been sufficiently well characterized to completely account for these increases.[9] The continuing accumulation of N_2O, which has an atmospheric lifetime of 120 to 150 years, is of concern for two reasons. Nitrous oxide has a climatic forcing factor 315 times as great as CO_2.[10] It is also the primary mechanism for the indirect delivery of nitric oxide into the stratosphere. The NO formed by reaction of N_2O with $O(^1D)$ constitutes a significant stratospheric ozone sink because NO catalyzes the $O_3 + O(^1D) \rightarrow 2O_2$ reaction.[11]

Microbial respiration yields large quantities of nitrous oxide by both nitrification ($NH_4^+ \rightarrow NO_3^-$) and denitrification ($NO_3^- \rightarrow NO, N_2O, N_2$) pathways;[12] the combined action of terrestrial and oceanic bacteria represents the dominant source term in

[⊗] Abstract published in *Advance ACS Abstracts*, February 1, 1997.

(1) Iwamoto, M.; Yahiro, H. *Catal. Today*.**1994**, *22*, 5−18.
(2) Armor, J. N. In *Environmental Catalysis*; Armor, J. N., Ed.; American Chemical Society: Washington, DC, 1994; Vol. 552, pp 2−6.
(3) Reed, J.; Eisenberg, R. *Science* **1974**, *184*, 568−70.
(4) Kudo, A.; Steinberg, M.; Bard, A. J.; Campion, A.; Fox, M. A.; Mallouk, T. E.; Webber, S. E.; White, J. M. *J. Catal.* **1990**, *125*, 565−567.
(5) Kubota, M.; Evans, K. J.; Koerntgen, C. A.; Marsters, J. C. J. *J. Mol. Catal.* **1980**, *7*, 481.
(6) Eisenberg, R.; Meyer, C. D. *Acc. Chem. Res.* **1975**, *8*, 26−34.
(7) Sun, K. S.; Kong, K. C.; Cheng, C. H. *Inorg. Chem.* **1991**, *30*, 1998−2004.
(8) Kubota, M.; Evans, K. J.; Koerntgen, C. A.; Marsters, J. C. *J. Am. Chem. Soc.* **1978**, *100*, 342−343.
(9) Thiemens, M. H.; Trogler, W. C. *Science* **1991** *251*, 932−934.
(10) Albritton, D.; Derwent, R.; Isaksen, I.; Lal, M.; Wuebbles, D. In *Climate Change 1995: The Science of Climate Change*; Houghton, J. T., Meira Filho, L. G., Callander, B. A., Harris, N., Kattenberg, A., Maskell, K., Eds.; Cambridge University Press: Cambridge, 1995; p 572.
(11) Crutzen, P. J.; Schmailzl, U. *Planet. Space Sci.* **1983**, *31*, 1009. Trogler, W. C. *J. Chem. Educ.* **1995**, *72*, 973−976.
(12) Delwiche, C. C. *Denitrification, Nitrification and Atmospheric Nitrous Oxide*; Wiley & Sons: New York, 1981.

S0002-7863(96)03588-3 CCC: $14.00

the global nitrous oxide budget.[13] Tolman and co-workers have prepared organic-soluble copper(I) complexes[14−16] that serve as functional models for the biologically relevant reduction of nitric oxide to nitrous oxide, but the metal-catalyzed aqueous reduction of NO is still poorly understood. Catalytic mechanisms that lead to nitrous oxide formation in aqueous environments may serve as models for elucidating the metalloenzymatic biochemistry of NO. In a previous paper $[PdCl_3NO]^{2-}$ was identified as the dominant species present under Wacker-type catalytic NO reduction conditions.[17] Kinetic details of the aqueous nitric oxide reduction step are reported herein.

Experimental Section

All reactions were performed with standard Schlenk techniques. UV/vis spectra were recorded in 1.0-cm quartz cells with the use of an HP 8452A diode array spectrometer. IR data were acquired at 2-cm^{-1} resolution with a Nicolet 510 FTIR spectrometer fitted with a MCT liquid-nitrogen-cooled detector. Pyrex cells with CaF_2 windows and 5 or 10 cm path lengths were used for gas sampling; a 0.1 mm path length cell with CaF_2 windows was used for spectra in D_2O.

Pd metal, $PdCl_2$, D_2O, NaCl, and HCl were used as received. Cylinders of CO (Linde, 99% minimum purity) and NO (Liquid Air, 99% minimum purity) were used as gas sources; the NO was spectroscopically free (<10 ppm) of higher nitrogen oxides. Liquid nitrogen boil-off supplied gaseous N_2. Cuprous chloride was prepared according to the published procedure.[18] Aqueous solutions were prepared with degassed HPLC-grade water.

IR Spectroscopic Analysis of $[PdCl_3NO]^{2-}$. A solution of 0.2019 g (1.14 mmol) of $PdCl_2$, 0.2032 g (2.05 mmol) of CuCl, and 1.2168 g (20.8 mmol) of NaCl was prepared in 10.0 mL of D_2O under N_2. After 30 min, the N_2 atmosphere was evacuated and replaced with 850 Torr of NO. The solution was agitated for 4 min before sampling. Data were collected at both 2- and 8-cm^{-1} resolutions (16 and 256 scans, respectively). Spectral subtraction was used to remove the background D_2O signal.

General Kinetics Protocol. Carefully weighed quantities of $PdCl_2$ and CuCl were dissolved in N_2-saturated 2.0 M HCl to prepare the standard solutions, which were shielded from light before use. For each run, 4.0 mL of solution was added to the quartz reaction chamber of the cell depicted in Figure 1. The solution was degassed under vacuum and isolated. The headspace IR chamber was pressurized with NO and sealed.

Reactions were performed within a temperature-controlled coldroom maintained at 20.0 ± 0.5 °C. Before initiating each kinetics run, the solution was thermally equilibrated in a water bath. Time zero for the reaction was determined by opening the stopcock, which allowed the NO to expand into the reaction chamber and mix with the aqueous solution. The cell was vigorously agitated on a vortex mixer for the duration of the experiment. UV/vis spectra (190−820 nm) were integrated for 1 s; one spectrum was recorded every 120 s for 30 min. Preliminary experiments were conducted to ensure that the mass transfer rate of NO into solution was faster than the rates measured.

Reaction rates were determined by following the formation of Cu(II) at 820 nm. All copper calibration standards were prepared in 2.0 M HCl, because the extinction coefficient of $CuCl_2$ was sensitive to the total chloride concentration. Formation of the catalytically active $[PdCl_3NO]^{2-}$ species takes place during the first 30−45 s of the reaction. As this complex has a broad absorption centered near 700 nm, the production of cupric chloride could not be readily determined from the absorbance values at 820 nm during this period. Once the intermediate species achieved a steady-state concentration, the baseline stabilized and subsequent increases at 820 nm were solely attributable to elevated Cu(II) concentrations. Rates of reaction were determined by quantifying the increase in $CuCl_2$ concentration as a function of time after a stable baseline had been established. CuCl slowly reduces NO to N_2O in the absence of palladium (*vide infra*). This secondary rate was also quantified and subtracted from the raw rate data to remove its influence. Appropriate techniques for determining the background corrections are detailed in the Results and Discussion section below. Error estimates for the linear regression analyses are reported at one standard deviation.

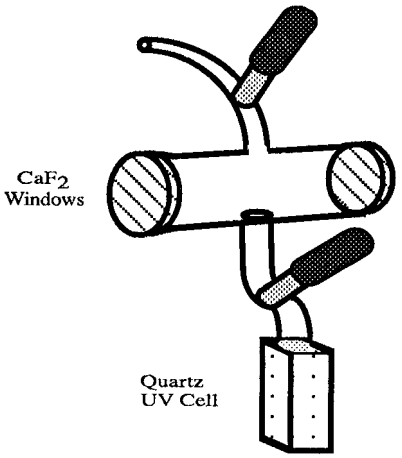

Figure 1. Reaction vessel used for kinetics experiments. Cell design permitted determination of solution-phase UV/vis spectra and the gaseous composition of the headspace by IR analysis. The large headspace volume also ensured that P_{NO} remained nearly invariant for the short duration of the kinetics experiments.

Results and Discussion

Previous studies of the catalytic reduction of nitric oxide by carbon monoxide under Wacker-type conditions (eqs 3−6) showed that the oxidation of CO to CO_2 precedes the reduction of N_2O.[5] This implies that the reactions of CO and NO are mechanistically independent. The generation of a spectroscopic intermediate with a λ_{max} of 436 nm was always observed during catalysis.[5] Formation of this intermediate required the simultaneous presence of $(PdCl_4)^{2-}$, CuCl, and NO. It was proposed initially that the catalytic species may be a mixed-metal multinuclear nitrosyl complex incorporating both palladium and copper.[5] It has been shown subsequently that a species with the identical spectroscopic and chemical features can be prepared in the absence of copper, and formulated as $[PdCl_3NO]^{2-}$.[17]

Based on these observations, we propose that the oxidation of carbon monoxide reduces the Pd(II) to Pd(0) (eq 3), which is then reoxidized predominately by Cu(II) (eq 5 ≫ eq 4). This accounts for the rapid formation of CO_2 and relatively sluggish initial N_2O generation. As Cu(I) accumulates in solution the rate of eq 7 increases and nitrous oxide production accelerates. The copper(II)/nitrous oxide stoichiometry was confirmed by allowing the reaction to proceed to completion in the cell depicted in Figure 1. Final concentrations of both products conformed to the stoichiometry of eq 7, with Cu(II):N_2O ratios of 1.9 (±0.2):1.

$$2NO + 2CuCl + 2HCl \xrightarrow{[PdCl_4]^{2-}} N_2O + 2CuCl_2 + H_2O \quad (7)$$

Although the oxidation of CO to CO_2 under Wacker-type

(13) Bouwman, A. F.; Fung, I.; Matthews, E.; John, J. *Global Biogeochem. Cycles* **1993**, *7*, 557−597.

(14) Ruggiero, C. E.; Carrier, S. M.; Tolman, W. B. *Angew. Chem., Int. Ed. Engl.* **1994**, *33*, 895−897.

(15) Ruggiero, C. E.; Carrier, S. M.; Tolman, W. B.; Antholine, W. E.; Whittaker, J. W.; Cramer, C. J. *J. Am. Chem. Soc.* **1993**, *115*, 11285−11298.

(16) Mahapatra, S.; Halfen, J. A.; Tolman, W. B. *J. Chem. Soc., Chem. Commun.* **1994**, 1625−1626.

(17) MacNeil, J. H.; Gantzel, P. K.; Trogler, W. C. *Inorg. Chim. Acta* **1995**, *240*, 299−304.

(18) Keller, R. N.; Wycoff, H. D. *Inorg. Synth.* **1946**, *2*, 1−4.

(19) Gruzinskaya, N. G.; Dzhumakaeva, B. S.; Golodov, V. A. *Kinet. Catal.* **1995**, *36*, 191−195.

Scheme 1

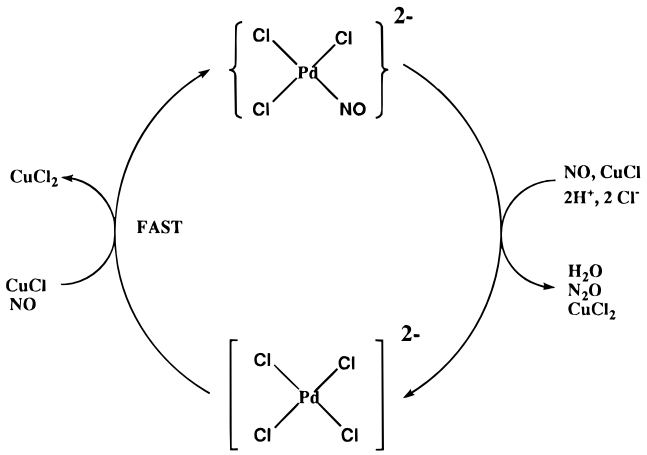

conditions has been studied extensively,[19] the mechanistic details of eq 7 were unknown. Therefore, attention was focused on the kinetics underlying nitric oxide reduction.

Formation of the Catalytic Intermediate. The $[PdCl_3NO]^{2-}$ species forms immediately after adding NO to a HCl solution of $[PdCl_4]^{2-}$ and $CuCl_2^-$. Rapid initial generation of Cu(II) is observed while $[PdCl_3NO]^{2-}$ appears; the rate of Cu(II) generated by subsequent catalytic turnover is an order of magnitude slower. A 1:1 Pd:Cu(II) ratio was determined for the initial generation of $[PdCl_3NO]^{2-}$.[17] Other data demonstrated a 1:1 Pd:NO ratio for this step, leading to the following reaction stoichiometry for formation of the catalytically active species:

$$[PdCl_4]^{2-} + NO + [CuCl_2]^- \rightarrow [PdCl_3NO]^{2-} + CuCl_2 + Cl^- \quad (8)$$

Although $[PdCl_3NO]^{2-}$ was too unstable to be isolated from 2 M HCl, its dimeric analog $[Pd_2Cl_4(NO)_2]^{2-}$ and the analogous nitro complex $[Pd_2Cl_4(NO_2)_2]^{2-}$ were prepared in dichloromethane.[17] Such dimeric species often form when chloropalladium(II) complexes are crystallized with bulky counterions from nonaqueous solutions. Significant differences between the UV/vis spectra of $[Pd_2Cl_4(NO)_2]^{2-}$ in CH_2Cl_2 (λ_{max} at 582 nm) and the intermediate present during aqueous catalysis (λ_{max} at 436 nm) suggested that eq 9 is shifted far to the right in HCl solution.[17] Additionally, the infrared spectrum of $[Pd_2Cl_4(NO)_2]^{2-}$ (in CH_2Cl_2) has two distinct absorptions at 1701 and 1623 cm^{-1}.[17] These presumably arise from symmetric and asymmetric NO stretches. In contrast, the aqueous palladium nitrosyl intermediate has a sharp feature at 1662 cm^{-1} (in D_2O), which is consistent with a monomeric formulation.

$$[Pd_2Cl_4(NO)_2]^{2-} + 2Cl^- \rightleftarrows 2[PdCl_3NO]^{2-} \quad (9)$$

To further test this hypothesis $[PdCl_3NO]^{2-}$ was generated in neutral solutions containing NaCl as a chloride source. Rapid evacuation of gaseous nitric oxide, followed by the introduction of oxygen into the headspace, led to the clean conversion of $[PdCl_3NO]^{2-}$ to $[PdCl_3(NO_2)]^{2-}$, with a λ_{max} of 406 nm. An isobestic point at 430 nm was observed for this transformation. The addition of 1 equiv of sodium nitrite to a solution of $[PdCl_4]^{2-}$ in 2 M NaCl produced $[PdCl_3(NO_2)]^{2-}$ (λ_{max} at 406 nm) by metathesis and confirmed the assignment.

Based on these data, the reaction pathway of Scheme 1 was developed, where $[PdCl_4]^{2-}$ first reacts rapidly with NO and Cu(I) to generate $[PdCl_3NO]^{2-}$. This intermediate species then reacts in a slower, rate-determining step with an additional equivalent of NO and Cu(I), as well as with two protons, to yield the final products and recycle $[PdCl_4]^{2-}$. Equation 10 depicts the stoichiometry of this latter step, whose kinetics are now examined.

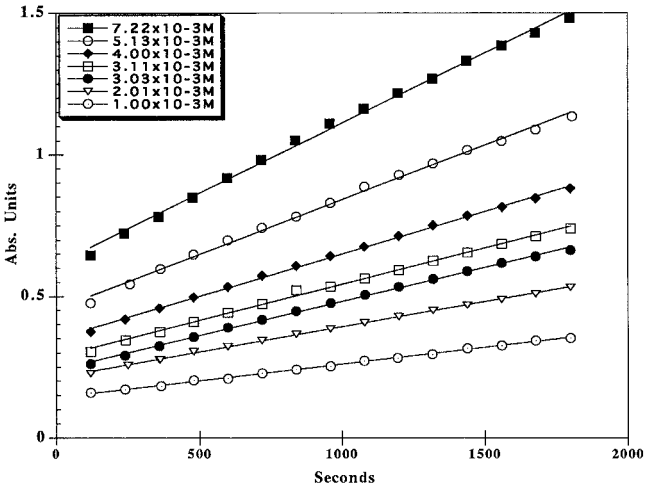

Figure 2. Initial rate data collected at a variety of $[PdCl_4]^{2-}$ concentrations, with $[CuCl_2]^-$ at 0.10 M and P_{NO} at 865 Torr. The plot shows the change in Cu(II) absorbance at 820 nm as a function of time. The absorbance at time zero is due to $[PdCl_3NO]^{2-}$ and increases in proportion to the original concentration of $[PdCl_4]^{2-}$. All data were collected at 20.0 ± 0.5 °C.

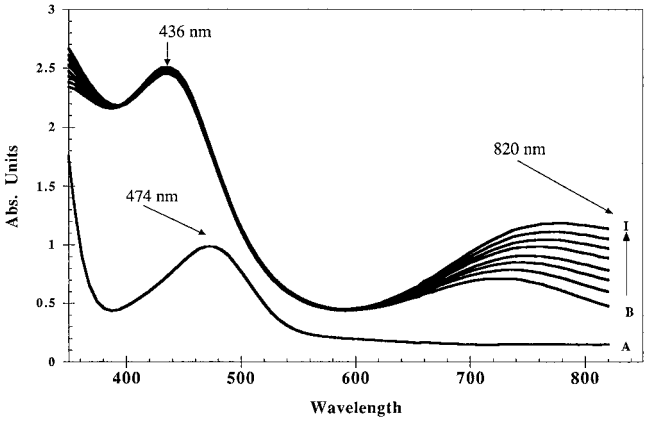

Figure 3. UV/vis spectra recorded for the first 30 min of a kinetic run containing 3.03×10^{-3} M $[PdCl_4]^{2-}$, 0.10 M $[CuCl_2]^-$, and 865 Torr of P_{NO} in 2 M HCl. Spectrum A was recorded before mixing the NO with the aqueous solution. The peak at 474 nm is that of $[PdCl_4]^{2-}$. Spectra B through I were recorded at 4-min intervals after introducing the NO. The band centered at 436 nm is from the $[PdCl_3NO]^{2-}$ intermediate. The increasing intensity at 820 nm in spectra B−I is due to increasing $CuCl_2$ concentration.

$$[PdCl_3NO]^{2-} + NO + 2HCl + CuCl_2^- \rightarrow N_2O + H_2O + [PdCl_4]^{2-} + CuCl_2 + Cl^- \quad (10)$$

General Kinetic Observations. All kinetics data were recorded using the method of initial rates. The concentration of Cu(I) was the limiting factor, and in most instances no more than 15% of the Cu(I) was consumed during the first 30 min. The rate of increase of Cu(II) as a function of time was linear over this range. Figure 2 depicts the initial rate data for a range of palladium concentrations. A small degree of curvature can be observed in the most concentrated solutions, when sufficient Cu(I) has been consumed to impinge on the pseudo-first-order excess of this reagent. Initial rates were extracted from the first 20 min of reaction when curvature was evident. Because 1 equiv of Cu(I) is oxidized to Cu(II) in a fast step to regenerate

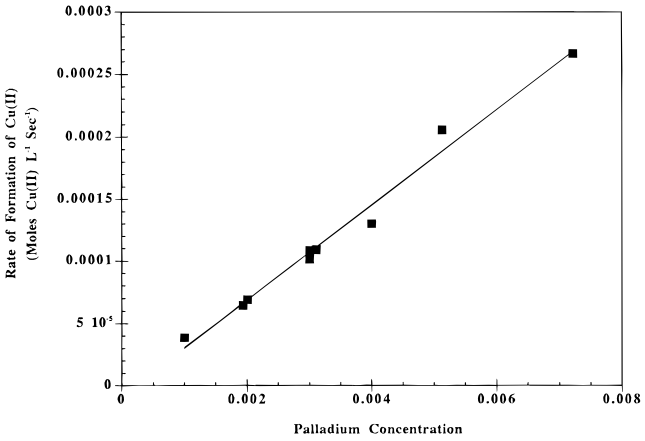

Figure 4. Plot of the corrected rates of Cu(II) formation as a function of the $[PdCl_4]^{2-}$ concentration at 20.0 ± 0.5 °C, with $[CuCl_2]^-$ at 0.100 M and P_{NO} at 865 Torr.

$[PdCl_3NO]^{2-}$ from $[PdCl_4]^{2-}$ (eq 8), only one-half of the total Cu(II) produced is attributed directly to the rate-determining step. Observed rates were divided by two to obtain the rate for the N_2O-forming step.

Data analysis also included the assumption that the formation rate of $[PdCl_3NO]^{2-}$ was much faster than its subsequent reaction to generate products. Hence the concentration of $[PdCl_3NO]^{2-}$ could be approximated by the total palladium concentration. This approximation is supported experimentally by the spectra in Figure 3 over the course of a 30-min reaction. The increase in Cu(II) concentration is apparent at 820 nm, while the λ_{max} for $[PdCl_3NO]^{2-}$ at 436 nm remains constant. Since the molar extinction coefficient for $[PdCl_3NO]^{2-}$ at 436 nm is 30 times larger than that of $CuCl_2$ at 820 nm in 2 M HCl, the $[PdCl_3NO]^{2-}$ concentration must be nearly invariant throughout the course of the experiment.

A complication in the analysis of the results was the slow reaction between CuCl and NO that occurs in the absence of palladium.[20] Equation 11 has the same copper/nitrous oxide stoichiometry as eq 7, but proceeds more slowly.

$$2CuCl + 2NO + 2HCl \rightarrow 2CuCl_2 + N_2O + H_2O \quad (11)$$

The rate of this background reaction was measured under conditions appropriate to each set of experiments and subtracted from the total observed rate. The background reaction comprised about 10% of the total rate at high concentrations of Pd, and about 35% at the lowest concentration of $[PdCl_4]^{2-}$ used. During experiments to determine the P_{NO} dependence, the background reaction comprised 10−15% of the overall experimental rate.

Palladium-Dependent Kinetics. Standard solutions were prepared in 2.0 M HCl containing 0.10 M CuCl. The headspace was initially charged with 970 Torr of NO, which dropped to 865 Torr after volume expansion into the reaction chamber at time zero. The palladium dependence was determined over the range $1-8 \times 10^{-3}$ M. At concentrations below this range, the rate was too slow to distinguish it accurately from the background reaction. Above the high end of the range the concentration of $[PdCl_3NO]^{2-}$ was no longer invariant, which is attributed to its rate of depletion approaching the mass transfer rate of NO into solution.

Plotting the corrected rates of Cu(II) formation as a function of palladium concentration yields a straight line (Figure 4) with a k_{obs} of (0.038 ± 0.002) s^{-1}. First-order kinetic dependence on the palladium concentration was further confirmed by a plot of log ([Pd(II)]) versus log (initial rate), as shown in Figure 5. The slope of this plot was 1.01 ± 0.04, which correlates well with first-order kinetics.

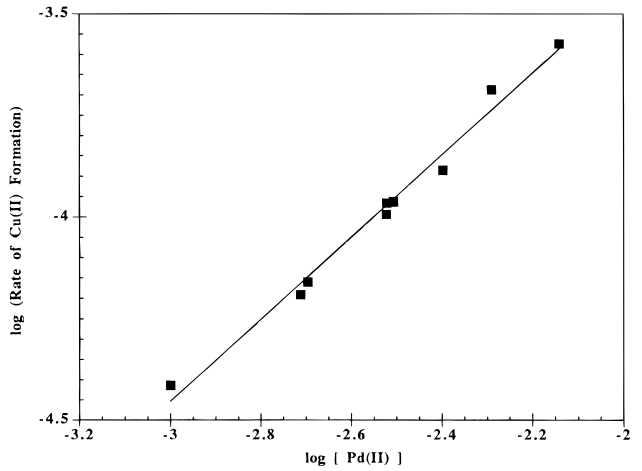

Figure 5. Plot of log $[Pd(II)]_{total}$ versus log [corrected rate of Cu(II) formation]. The slope of the line was 1.01 ± 0.04, indicative of first-order kinetic behavior.

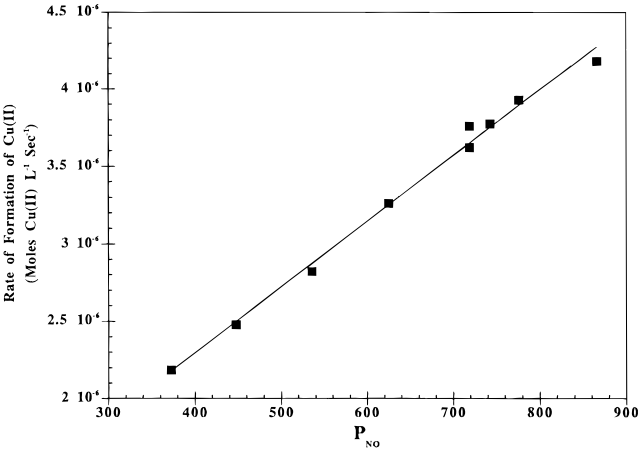

Figure 6. Plot of the corrected rates of Cu(II) formation as a function of P_{NO} (Torr), 20.0 ± 0.5 °C, with $[PdCl_4]^{2-}$ at 3.0×10^{-3} M and $[CuCl_2]^-$ at 0.10 M.

***P*$_{NO}$ Dependent Kinetics.** Experiments to determine the nitric oxide dependence were conducted with standard solutions of 3.0×10^{-3} M $PdCl_2$ and 0.10 M CuCl in 2.0 M HCl. A bulk solution was prepared each day, as Cu(I) is not stable indefinitely in acidic aqueous media. The headspace reservoir was loaded with NO before each experiment and then adjusted to 970 Torr with nitrogen. Nitric oxide partial pressures from 865 to 350 Torr (after expansion) were investigated. At lower NO pressures the UV/vis spectra indicated that formation of $[PdCl_3NO]^{2-}$ did not go to completion. This was evidenced by lower absorbance values and a bathochromic shift in λ_{max}.

Blank values for this set of reactions were determined by reacting 0.10 M CuCl solutions in 2.0 M HCl at a series of NO partial pressures. The equation derived from a linear regression analysis of these data was then used to calculate the correction factor appropriate for each experimental point determined during the catalytic measurements. A plot of P_{NO} versus the initial rate of Cu(II) formation was linear over the range of partial pressures studied, as depicted in Figure 6. A k_{obs} value of (4.2 ± 0.1) $\times 10^{-9}$ s^{-1} was determined from the slope of this plot.

Cu(I) Dependent Kinetics. The kinetic dependence on the initial concentration of Cu(I) was investigated in the range between 0.01 and 0.2 M CuCl. Standard solutions 3.0×10^{-3} M in $PdCl_2$ were prepared by two different techniques. To help

(20) Nunes, T. L.; Powell, R. E. *Inorg. Chem.* **1970**, *9*, 1912−6.

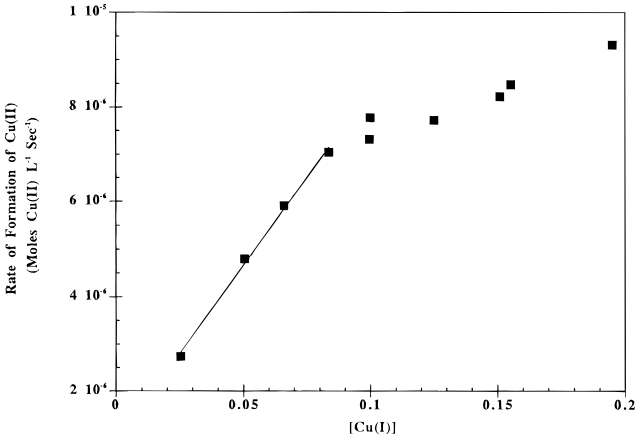

Figure 7. Plot of the corrected rates of Cu(II) formation as a function of the Cu(I) concentration, 20.0 ± 0.5 °C, $[PdCl_4]^{2-}$ at 3.0×10^{-3} M, and P_{NO} at 865 Torr.

maintain a constant concentration of $PdCl_2$, bulk solutions of palladium were prepared in 2.0 M HCl, and CuCl was then added to achieve the desired concentration. All experiments were performed with 865 Torr of NO. The background reactions of some experiments were calculated by preparing a calibration curve over the range of copper concentrations and interpolating the palladium-free rate from the resultant data. Other samples were prepared by dissolving CuCl in 2.0 M HCl, then adding $PdCl_2$ to half of the solution. This allowed the background rate to be measured at the same copper concentration as the palladium-catalyzed rate. Both methods yielded comparable results and were merged to form the complete data set. Sodium chloride was added to compensate for reduced concentrations of CuCl.

The data for the Cu(I) dependence were more complicated than those above. Below approximately 0.1 M the dependence was linear and first order in Cu(I). Above 0.1 M Cu(I), a distinct deviation from first-order behavior is observed (Figure 7). Further increasing the concentration of Cu(I) gave a limiting rate, indicative of saturation kinetics. The rates of reaction in these experiments were slow enough to exclude NO mass transfer as a possible cause of the observed saturation. A k_{obs} value of $(7.4 \pm 0.3) \times 10^{-5}$ s^{-1} was determined from the first-order portion of the data.

H^+ and Cl^-- Dependent Kinetics. Standard solutions of $PdCl_2$ and CuCl were combined with 865 Torr of NO to evaluate the rate-determining step's dependence on acidity. Acid concentrations between 0.20 and 2.0 M were tested; NaCl was substituted to maintain the ionic strength. The rate of reaction was found to be independent of acidity over the range of concentrations studied. Quantitative analysis of the kinetic dependence on chloride concentration was hampered by the lack of a suitable anion that was chemically inert and did not alter the acidity of the solution. Qualitative observations are consistent with previous reports, in which the HCl concentration was varied over the range 2−4 M without affecting the rate of reaction.[5] This suggests that chloride is required primarily to ligate and solubilize CuCl (as $CuCl_2^-$) and $PdCl_2$ (as $[PdCl_4]^{2-}$).

Mechanistic Hypothesis. Because of the distinct similarities in the reaction conditions, it has been convenient to fashion a model for the Pd(II)/Cu(I) catalysis of eq 1 after the well-established Wacker mechanism for the oxidation of olefins.[21] Such a comparison does not yield useful mechanistic insight for the current system. The stoichiometric reduction of nitric oxide is zero order in chloride and proton concentrations, while the Wacker oxidation of olefins is strongly inhibited by both components.[21] A valid mechanistic interpretation of the present data must also account for the first-order dependencies on $PdCl_2$ and NO, and the saturation behavior of Cu(I).

One route proposed for the metal-catalyzed reduction of nitric oxide to nitrous oxide involves initial formation of a *cis*-dinitrosyl complex.[22] The two nitrosyl ligands couple and are reduced to form hyponitrite $(N_2O_2)^{2-}$, which subsequently reacts with protons to generate H_2O and N_2O. Moser explored the solid-state thermal decomposition of many metal dinitrosyls,[23] and the $M(NO)_2$ motif has also been identified as playing a role in the homogeneous, solution-phase reduction of NO to N_2O for a variety of transition metals, including Rh,[24,25] Ir,[26] Ru,[27] Fe,[28] and Pt.[29] An analogous mechanism incorporating the components of the present system might be envisioned to proceed via Scheme 2.

The first step in Scheme 2 would involve exchange of a second chloride ligand for a nitrosyl ligand. This suggests that the rate of reaction should be inhibited by excess chloride. This is inconsistent with the current data and prior observations, which are independent of Cl^- concentration.

An alternative explanation (Scheme 3) might involve a pre-equilibrium between Cu(I) and NO, and delivery of NO^- by an associative pathway. There are several experimental observations that exclude this option. Cuprous chloride serves as a carbon monoxide transfer agent for the carbonylation of $[PtCl_4]^{2-}$; however, a negative first-order dependence on chloride concentration was observed for this process.[7] There was no spectroscopic (UV/vis) evidence of a Cu(I)−NO complex either in the platinum study[30] or in the current palladium experiments. Finally, the sequence of reactions of Scheme 3 fails to explain the saturation kinetics observed for Cu(I), effectively eliminating it from consideration.

For these reasons, alternative mechanisms were considered. It is known that bent nitrosyl ligands are subject to electrophilic attack at the nitrogen lone pair.[22] While X-ray structural data of $[PdCl_3NO]^{2-}$ are unavailable, the low-frequency ν_{NO} IR stretch at 1662 cm^{-1} (D_2O) is indicative of a bent nitrosyl geometry.[31] Several examples of electrophilic attack of free nitric oxide on a bound nitrosyl ligand have been reported. It has been shown that $Co(en)_2(NO)Cl_2$ undergoes disproportionation to generate $Co(en)_2(NO_2)Cl_2$ and N_2O,[32] and that $[Co(NO)(NH_3)_5]^{2+}$ also reacts with free NO to generate the asymmetric hyponitrite-bridged dimer of Scheme 4.[33]

Evidence of a disproportionation mechanism in the Pd(II)/Cu(I) chemistry is lacking. Detectable quantities of coordinated chloronitropalladium species were not observed. Furthermore, nitrous acid that would be formed by protonation of a nitro

(21) Henry, P. M. In *Advances in Chemistry Series (Homogeneous Catalysis)*; Luberoff, B. J., Ed.; American Chemical Society: Washington, DC, 1970. Zaw, K.; Henry, P. M. *Organometallics* **1992**, *11*, 2008−2015.

(22) Eisenberg, R.; Hendriksen, D. E. *Adv. Catal.* **1979**, *28*, 79−172.

(23) Moser, W. R. In *The Catalytic Chemistry of Nitric Oxides*; Plenum Press: 1975; pp 33−43.

(24) Hendriksen, D. E.; Meyer, C. D.; Eisenberg, R. *Inorg. Chem.* **1977**, *16*, 970.

(25) Kaduk, J. A.; T. H., T.; Budge, J. R.; Ibers, J. A. *J. Mol. Catal.* **1981**, *12*, 239−243.

(26) Haymore, B. L.; Ibers, J. A. *J. Am. Chem. Soc.* **1974**, *96*, 3325−7.

(27) Bhaduri, S.; Johnson, B. F. G. *Transition Met. Chem.* **1978**, *3*, 156−161.

(28) Pearsall, K. A.; Bonner, F. T. *Inorg. Chem.* **1982**, *21*, 1978−1985.

(29) Bhaduri, S.; Johnson, B. F. G.; Savory, C. J.; Segal, J. A.; Walter, R. H. *J. Chem. Soc., Chem. Commun.* **1974**, 809.

(30) Sun, K. S.; Kong, K. C.; Cheng, C. H. *Inorg. Chem.* **1991**, *30*, 1998−2004.

(31) Legzdins, P.; Richter-Addo, G. B. *Metal Nitrosyls*; Oxford University Press: New York, 1992; p 369.

(32) Gwost, D.; Caulton, K. G. *Inorg. Chem.* **1974**, *13*, 414−417.

(33) Hoskins, B. F.; Whillans, F. D.; Dale, D. H.; Hodgkin, D. C. *Chem. Commun.* **1969**, 69.

Scheme 2

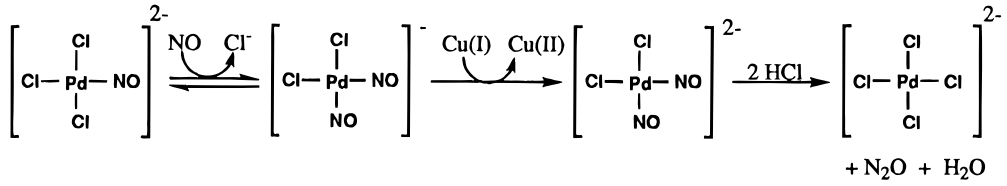

Scheme 3

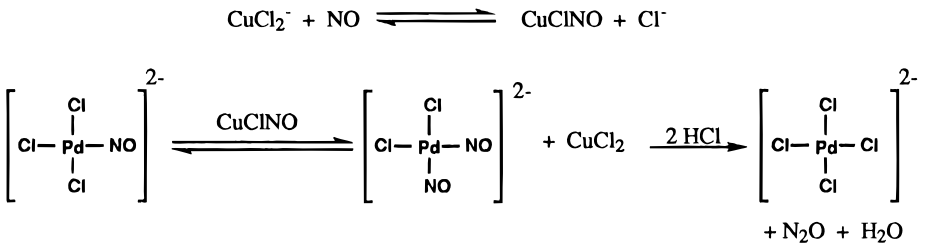

Scheme 4

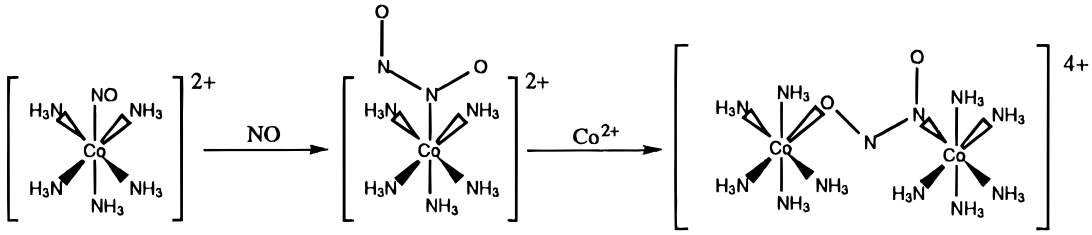

Scheme 5

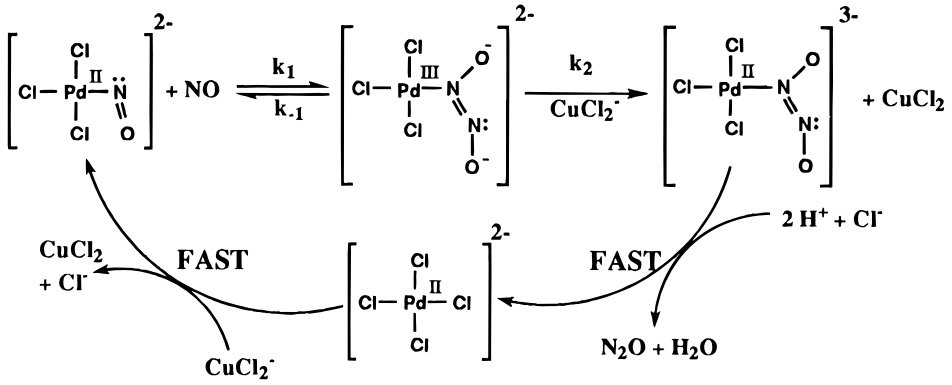

complex is unstable and disproportionates into NO and NO_3^- in acidic solutions. Nitrate was not detectable as a reaction product, yet it is stable under the conditions of the catalysis. Finally, the stoichiometry of the disproportionation reaction (eq 12) does not correspond to the experimentally determined 2:1 Cu(II):N_2O stoichiometry of eq 7.

$$2H^+ + 3Cu^+ + 7NO \xrightarrow{PdCl_2} 3N_2O + NO_3^- + 3Cu^{2+} + H_2O \quad (12)$$

The NO reduction mechanism that best represents the reaction stoichiometry and kinetics of the Pd(II)/Cu(I) system is depicted in Scheme 5. In this scheme, the nitrosyl ligand undergoes reversible electrophilic attack at the nitrogen lone pair by free nitric oxide from the bulk solution. This generates a low, steady-state concentration of an intermediate that is reduced by Cu(I). The electron provided permits loss of $(N_2O_2)^{2-}$, which is known to rapidly decompose to N_2O, and regenerates Pd(II). Although the formation of the $[Cl_3Pd(N_2O_2)]^{2-}$ intermediate is presumed to originate from electrophilic attack of free NO on the lone pair of the nitrosyl ligand, the kinetics data cannot exclude the initial, transitory formation of a five-coordinate palladium dinitrosyl that rapidly rearranges to $[Cl_3Pd(N_2O_2)]^{2-}$.

Applying the steady-state approximation to the $[PdCl_3(N_2O_2)]^{2-}$ intermediate in Scheme 5 yields the following expression:

$$\text{rate} = \frac{\text{d(products)}}{\text{d}(t)} = \frac{k_1 k_2 [\text{Pd}_t] P_{\text{NO}} [\text{Cu(I)}]}{k_{-1} + k_2 [\text{Cu(I)}]}$$

This rate expression can be inverted to produce the following two-term equation.

$$\frac{1}{\text{rate}} = \frac{k_{-1}}{k_1 k_2 [\text{Pd}_t] P_{\text{NO}} [\text{Cu(I)}]} + \frac{1}{k_1 [\text{Pd}_t] P_{\text{NO}}}$$

A plot of rate^{-1} versus [Cu(I)]$^{-1}$ provides a slope of $k_{-1}/(k_1 k_2 [\text{Pd}_t] P_{\text{NO}})$ and an intercept equal to $1/(k_1 [\text{Pd}_t] P_{\text{NO}})$. Figure 8 shows a plot of these data derived from the Cu(I)-dependence experiments. When [Pd$_t$] and P_{NO} are held constant (at 3.0×10^{-3} M and 865 Torr, respectively) a value of $k_1 = ((6.0 \pm 0.4) \times 10^{-6})(P_{\text{NO}})^{-1}$ s^{-1} at 20 °C is obtained. The ratio $(k_{-1})/(k_2)$ yields a value of 0.116 ± 0.004 M. Because the back reaction

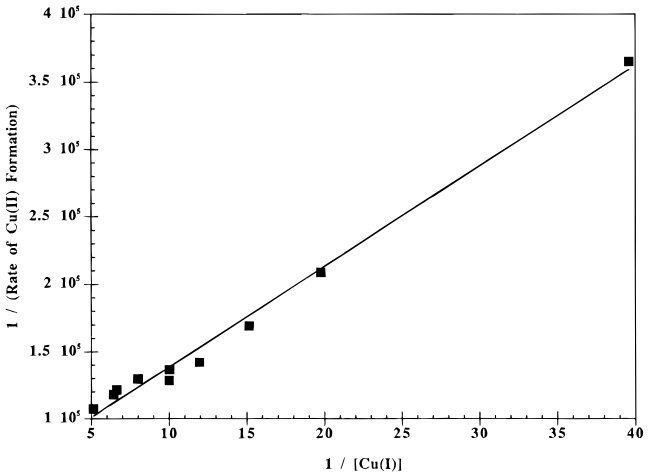

Figure 8. Plot of [corrected rate of Cu(II) formation]$^{-1}$ versus [Cu(I)]$^{-1}$ from the data recorded for the Cu(I) dependence in Figure 7.

k_{-1} is unimolecular while the forward reaction k_2 is bimolecular, it is more informative to note that $(k_{-1})/(k_2)$[Cu(I)] = 1.16 at 0.10 M CuCl. The intermediate formed by attack of NO on $[PdCl_3NO]^{2-}$ is subsequently reduced by Cu(I) slightly less than half the time.

To test whether the kinetics for the stoichiometric reduction of NO to N_2O represents the rate-determining step for the Wacker catalysis of eq 1, parallel experiments were conducted under catalytic conditions. When the atmosphere above a Pd(II)/Cu(II) solution was charged with 400 Torr of CO and 400 Torr of NO, the oxidation of CO to CO_2 predominated initially. Within about 20 min all the Cu(II) had been reduced to Cu(I) and a steady-state concentration was achieved. At this time $[PdCl_3NO]^{2-}$ accounted for almost all the initial palladium concentration. The rate of N_2O generation was linear from this point for at least the next 90 min, and was 93% of the reaction rate observed when the same cell was charged with 400 Torr of NO and 400 Torr of N_2 above a corresponding Pd(II)/Cu(I) solution. As some small quantity of palladium remains tied up in the steady-state oxidation of CO, the close agreement of the two experimental rates suggests that the stoichiometric NO reduction step primarily determines the rate of the full catalytic cycle.

Cheng et al. have reported a catalytic cycle that promotes the concomitant oxidation of CO and the reduction of NO, yielding CO_2 and N_2O, in the presence of $(PtCl_4)^{2-}$, Cu(I), and Cu(II).[30] It was shown that the CO oxidation mechanism was completely different than the reactions with palladium, and required nitric oxide to proceed. The reduction of NO was not examined mechanistically, but was represented by the following reaction (which was not rate-determining in their system).

$$[PtCl_2(NO)]^{2-} + NO + 2H^+ + 2Cl^- \rightarrow [PtCl_4]^{2-} + N_2O + H_2O \quad (13)$$

It was assumed that eq 13 might proceed by the reactions outlined in Scheme 2 above. The catalysis was performed in 0.6 M HCl and occupation of the fourth coordination site by chloride would generate $[PtCl_3NO]^{3-}$. Such a species should render the bound nitrosyl susceptible to electrophilic attack, and could generate nitrous oxide through a mechanism analogous to that proposed here (Scheme 5).

There is an apparent similarity between the Pd(II)/Cu(I) mechanism and that proposed for the nitric oxide reductase activity of cytochrome *c* oxidase (CcO). Nitrosyl ligation of CcO, hemoglobin, and myoglobin has long been known, but it has been reported recently that CcO promotes the two-electron reduction of NO to nitrous oxide by eq 14.[34]

Scheme 6

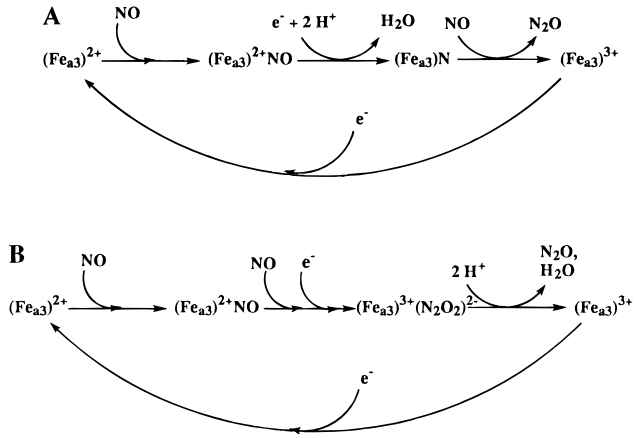

$$2NO + 2e^- + 2H^+ \rightarrow N_2O + H_2O \quad (14)$$

The enzyme-catalyzed reduction occurs through initial binding of nitric oxide to the reduced heme site $(Fe_{a3})^{2+}$ yielding a stable iron−mononitrosyl (υ_{NO} = 1610 cm^{-1}).[35] It was suggested that nitrogen−nitrogen bond formation takes place through reaction with a second nitrosyl bound to $(Cu_B)^+$,[35,36] but it has since been shown that the role of $(Cu_B)^+$ is that of a one-electron transfer agent. Furthermore, NO ligation on $(Cu_B)^+$ (who's affinity for NO is only half that of $(Fe_{a3})^{2+}$)[34] inhibits the NO reduction activity of CcO by weakening the electron-donating capacity of $(Cu_B)^+$.[34] The mechanism of scheme 6A was proposed by analogy to the route of O_2 oxidation, although a monomeric hemin nitride would be expected to be a high-energy intermediate. In contrast, the nucleophilic attack of free NO upon the coordinated nitrosyl ligand, as in Scheme 6B, would parallel the current palladium mechanism and those proposed previously for cobalt.[32,33,37] Reaction of protons with the hyponitrite moiety in Scheme 6B generates H_2O and N_2O by a well established pathway. Schemes 6A and 6B differ in the position of the mechanism's protonation step. It has been noted that the protons consumed during nitric oxide reductase activity are not of the same origin as those used in reducing O_2.[38] Thus, a NO reduction mechanism that completely parallels the O_2 case may not be warranted. Both pathways proposed in Scheme 6 are consistent with the retardation of the enzyme's NO reduction capacity when nitric oxide is coordinated to $(Cu_B)^+$, as both are initiated by a one-electron transfer assumed to originate at this site.

In 1989 Shoun and co-workers reported the first example of eukaryotic denitrification.[39] A unique type of cytochrome P450, denoted P450nor, was isolated from the fungus *Fusarium oxysporum*.[39] Cytochrome P450nor is capable of nitric oxide reductase activity but cannot catalyze the monooxygenase

(34) Zhao, X.-J.; Sampath, V.; Caughey, W. S. *Biochem. Biophys. Res. Commun.* **1995**, *212*, 1054−1060.
(35) Zhao, X.-J.; Sampath, V.; Caughey, W. S. *Biochem. Biophys. Res. Commun.* **1994**, *204*, 537−543.
(36) Brudwig, G. W.; Stevens, T. H.; Chan, S. I. *Biochemistry* **1980**, *19*, 5275−5285.
(37) Dorfman, Y. A.; Emel'yanova, V. S.; Zhusupbekov, B. O. *Kinet. Katal.* **1981**, *22*, 375−378.
(38) van der Oost, J.; de Boer, A. P. N.; de Gier, J-W. L.; Zumft, W. G.; Stouthamer, A. H.; van Spanning, R. J. M. *FEMS Microbiol. Lett.* **1994**, *121*, 1−10.
(39) Shoun, H.; Suyama, W.; Yasui, T. *FEBS Lett.* **1989**, *244*, 11−14. Shoun, H.; Tanimoto, T. *J. Biol. Chem.* **1991**, *266*, 11078−11082.

Scheme 7

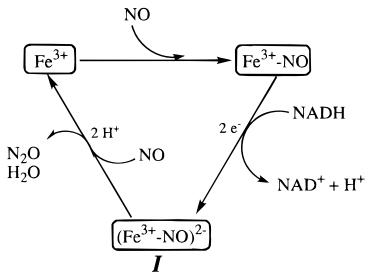

I

reaction.[40] The mechanism proposed for the reduction of NO to N_2O by this enzyme is outlined in Scheme 7.[40]

In this mechanism, the NO binds to the ferric heme and undergoes two-electron reduction to an intermediate species ***I***. In solutions sparged of excess NO this intermediate was observed to decay spontaneously much more slowly than the catalytic turnover rates determined when NO was present. This led the authors to propose that the reduced nitrosyl reacts with protons and NO to generate nitrous oxide and water.[40] It is known that the channel to the active site is large enough to accommodate a second nitric oxide molecule.[40] While a hyponitrite mechanism was thought to be biochemically unprecedented, it does have many features in common with the cytochrome *c* oxidase pathway proposed in Scheme 6B.

(40) Shiro, Y.; Fujii, M.; Iizuka, T.; Adachi, S-I.; Tsukamoto, K.; Nakahara, K.; Shoun, H. *J. Biol. Chem.* **1995**, *270*, 1617−1623.

Acknowledgment. We thank the National Science Foundation for support of this research through grants CHE-9216618 and CHE-9632311. T.L.P. and P.A.B. acknowledge the support of NSF REU fellowships. P.A.B. thanks the Howard Hughes program for providing additional funding.

JA963588B